JOURNAL OF SCIENCE
SAKARYA UNIVERSITY

Sakarya University Journal of Science

ISSN 1301-4048 | e-ISSN 2147-835X | Period Bimonthly | Founded: 1997 | Publisher Sakarya University | http://www.saujs.sakarya.edu.tr/

Title: Co-crystal of carbazole-based thiourea derivative compound with acetic acid: Crystallography and Hirshfeld surface analysis

Authors: Ilkay Gumus
Recieved: 2018-05-03 00:00:00

Accepted: 2018-12-20 00:00:00

Article Type: Research Article
Volume: 23
Issue: 3
Month: June
Year: 2019
Pages: 368-381

How to cite
Ilkay Gumus; (2019), Co-crystal of carbazole-based thiourea derivative compound with acetic acid: Crystallography and Hirshfeld surface analysis. Sakarya University Journal of Science, 23(3), 368-381, DOI: 10.16984/saufenbilder.420679
Access link
http://www.saujs.sakarya.edu.tr/issue/41686/420679

Sakarya University Journal of Science 23(3), 368-381, 2019

# Co-crystal of carbazole-based thiourea derivative compound with acetic acid: Crystallography and Hirshfeld surface analysis

Ilkay Gumus*[1]

**Abstract**

Co-crystal of the *N*,*N*′-(((3,6-dichloro-9*H*-carbazole-1,8-diyl)*bis*(azanediyl))*bis*(carbonothioyl))*bis*(2,2-dimethylpropanamide) as a carbazole-based thiourea derivative (CBT) with acetic acid (AcOH) was prepared and its molecular structure examined using the single crystal X-ray diffraction study and the Hirshfeld surface analysis. The co-crystal was designed to explore the supramolecular synthons and intermolecular interactions diversity between the components of co-crystal. The analysis of the crystal structure and packing revealed that the CBT:AcOH co-crystal are formed by a strong O–H···S and C-H···O hydrogen bonding interactions between components of co-crystal. In addition, its' structure is further stabilized by strong C-H···π stacking interactions and N-H···O and N-H···S homosynthons between CBT molecules. The Hirshfeld surfaces and associated two-dimensional fingerprint plots of the co-crystal were also analyzed to clarify the nature of the hydrogen bond interactions and close intermolecular interactions in the crystal structure. The Hirshfeld surfaces and the associated two-dimensional fingerprint plots analysis revealed that the majority of close contacts forming supramolecular structure were associated with relatively weak interactions such as H···H, C···H and N···H. So, it can be said that these interactions play a major role in molecular crystal packing.

**Keywords:** Carbazole-based thiourea derivative, Cocrystal, Hirshfeld surface analyses, Crystal structure, Non-covalent interactions.

## 1. INTRODUCTION

A molecular assembly where two or more compounds interact with each other *via* supramolecular interactions such as van der Waals, electrostatic, dipole-dipole, hydrogen bonding and C-H···π, π···π stacking interactions. Recently, supramolecular interactions have attracted considerable attention due to the utilization of intermolecular non-covalent interactions is relied upon for the design and advancement of functional materials [1-3]. The non-covalent interactions such as classical/non-classical hydrogen bonding, C-H···π, π···π stacking interactions, electrostatic and charge transfer interactions have been used in the self-assembly and design a large number of supramolecular architectures in solids [4-9]. Multi-component crystalline systems can be separated into co-crystals, solvates and salts. The co-crystal supramolecular structures are formed by supramolecular synthons, where molecular moieties are connected by intermolecular interactions that

* Corresponding Author

[1]Department of Chemistry, Faculty of Arts and Science, Mersin University, Mersin, TR 33343, Turkey. Tel: +90.538.5589656, Fax: +90.324.3610047, e-mail: ilkay.gumus@mersin.edu.tr ORCID: 0000-0002-9398-0057

provide useful information about the structure of crystals [10-12].

The co-crystals improve properties such as stability, solubility, dissolution rate and bioavailability of compounds due to the crystal lattice of co-crystals, which may include solvent and/or water molecules [13-15]. Therefore, co-crystal formation is a new strategy to improve the solubility and stability of non-ionizable drugs and industrial useful materials [16-18].
Recently, our research group focused on the carbazole derivatives which have useful biological properties such as antitumor, anti-inflammatory, antihistaminic and antibiotic [19,20]. In our ongoing research studies, we prepared a series of carbazole compounds. One of them is *N*,*N*′-(((3,6-dichloro-9*H*-carbazole-1,8-diyl)*bis*(azanediyl))*bis*(carbonothioyl))*bis*(2,2-dimethylpropanamide). This compound has been obtained in powder form. This compound could not be crystallized using solvents such as DMF, DMSO, MeCN and DCM due to its low solubility. Therefore, we did not obtain enough data to confirm the crystal and molecular structure of the prepared compound. So, we tried to obtain a crystal form by co-crystal preparation technique. We only obtained the proper quality crystaline form of this compound using acetic acid as solvate. That means, the addition of acetic acid contributed to the formation of co-crystal and increased the solubility. Therefore, we examined the supramolecular architecture in solid formed by co-crystallization of *N*,*N*′-(((3,6-dichloro-9*H*-carbazole-1,8-diyl)*bis*(azanediyl))*bis* (carbonothioyl))*bis*(2,2-dimethylpropanamide) with acetic acid and investigated the hydrogen bonding, C-H···π, π···π stacking interactions and synthons formed in the crystalline solid state. Moreover, we visualized and confirmed all these interactions using Hirshfeld surface analysis.

## 2. EXPERIMENTAL

### 2.1. Instrumentation

The NMR spectra were recorded in DMSO-$d_6$ solvent on Bruker Avance III 400 MHz NaNoBay FT-NMR spectrophotometer using tetramethyl-silane as an internal standard. For infrared spectra, each compound was recorded in the range 400-4000 $cm^{-1}$ on a Perkin Elmer Spectrum 100 series FT-IR/FIR/NIR Spectrometer Frontier, ATR Instrument.

The X-ray single crystal diffraction data were recorded on a Bruker APEX-II CCD diffrac-tometer. A suitable crystals was selected and coated with Paratone oil and mounted onto a Nylon loop on the diffractometer. The crystal was kept at $T$ = 100 K during data collection. The data were collected with MoKα (λ = 0.71073 Å) radiation at a crystal-to-detector distance of 40 mm. Using Olex2 [21], the structure was solved with the Superflip [22-24] structure solution program, using the Charge Flipping solution method and refined by full-matrix least-squares techniques on $F^2$ using ShelXL [25] with refinement of $F^2$ against all reflections. Hydrogen atoms were constrained by difference maps and were refined isotropically, and all non-hydrogen atoms were refined anisotropically.

### 2.2. Hirshfeld surfaces analysis

Analysis of Hirshfeld surfaces and their associated two-dimensional (2D) fingerprint plots of co-crystal were calculated using Crystal Explorer 3.1 [26]. The Hirshfeld surfaces mapped with different properties $d_{norm}$ and shape index. The $d_{norm}$ is normalized contact distance, defined in terms of $d_e$, $d_i$ and the van der Waals (vdW) radii of the atoms. The combination of $d_e$ and $d_i$ in the form of a 2D fingerprint plot displays summary of intermolecular contacts in the crystal.

### 2.3. Synthesis and characterization

Precursor materials 3,6-dichlorocarbazole (1), 3,6-dichloro-1,8-dinitrocarbazole (2) and 1,8-diamino-3,6-dichlorocarbazole (3) were prepared according to the previously published method [27-29].

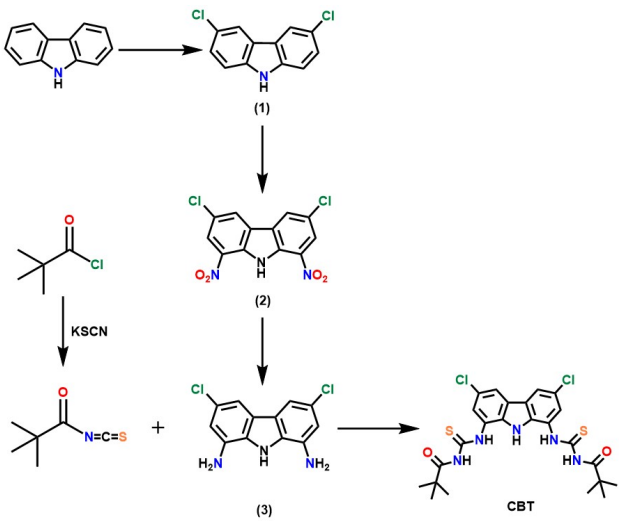


Scheme 1

### 2.3.1. Synthesis of 3,6-dichlorocarbazole (1)

The carbazole (5 g, 0.03 mol) and $CH_2Cl_2$ (500 mL) were added to a round-bottomed flask and cooled to 0 °C. Then, $SO_2Cl_2$ (19.2 mL, 0.24 mol) was added dropwise by vigorous stirring. After the addition, the cooling bath was removed and the reaction mixture was stirred for another 4 hours at room temperature. The solid precipitate was filtered off, washed with $CH_2Cl_2$ and dried (Scheme 1). Color: Pink. Yield: 75%. $^1$H NMR (400 MHz, DMSO-$d_6$, δ, ppm): 11.60 (s, 1H, NH), 8.31 (d, 2H, *J1* = 2.0 Hz, Ar-H), 7.54 (d, 2H, Ar-H), 7.44 (dd, 2H, *J1* = 8.6 Hz, *J2* = 2.0 Hz, Ar-H). $^{13}$C NMR (100 MHz, DMSO-$d_6$, δ, ppm): 138.7, 126.1, 123.2, 122.8, 120.3, 112.7. FT-IR (ATR, cm$^{-1}$): 3405 ν(NH), 3245, 3082 ν(Ar-CH), 803, 868 ν(C-Cl). LC-MS (-ESI, *m/z*): 202.2 [M-Cl]$^+$, 187.2, 167.3, 136.3, 111.0.

### 2.3.2. Synthesis of 3,6-dichloro-1,8-dinitro-carbazole (2)

3,6-Dichlorocarbazole (1) (7.08 g, 0.03 mol), acetic acid (20 mL) and acetic anhydride (15 mL) were added to a round-bottomed flask. The solution was then cooled to 1 °C and 100% $HNO_3$ (3.6 mL, 0.0875 mol) was added dropwise. Then, the cooling bath was replaced by an oil bath. The mixture was heated to 60 °C and kept at this temperature. The reaction mixture was further heated, until it reached 75 °C. Afterwards, the suspension was filtered while hot and the product was washed with boiling acetic acid (30 mL) and diethyl ether. (Scheme 1). Color: Yellow. Yield: 69%. $^1$H NMR (400 MHz, DMSO-$d_6$, δ, ppm): 11.28 (bs, 1H, NH), 8.98 (d, 2H, Ar-H), 8.48 (d, 2H, Ar-H). $^{13}$C NMR (100 MHz, DMSO-$d_6$, δ, ppm): 132.73, 132.01, 128.92, 125.79, 125.09, 123.32. FT-IR (ATR, cm$^{-1}$): 3454 ν(NH), 3088, 1617, 1518, 754. LC-MS (-ESI, *m/z*): 324.4 [M-2H]$^+$, 290.4, 264.4, 224.2, 195.2, 136.5, 111.2.

### 2.3.3. Synthesis of 1,8-diamino-3,6-dichloro-carbazole (3)

3,6-Dichloro-1,8-dinitrocarbazole (3) (2.00 g, 6.13 mmol) was dissolved in THF (50 mL) and 5% palladium on charcoal was added (0.2 g). The mixture was vigorously stirred under hydrogen atmosphere. The catalyst was filtered off on Celite after about 2 hours. The solvent was evaporated and the solid purified by crystallization from methanol. Color: Grey. Yield: 69%. $^1$H NMR (400 MHz, DMSO-$d_6$, δ, ppm): 10.67 (s, 1H, NH), 7.35 (d, 2H, Ar-H), 6.66 (d, 2H, Ar-H), 5.35 (s, 4H, $NH_2$). $^{13}$C NMR (100 MHz, DMSO-$d_6$, δ, ppm): 135.00, 127.38, 123.79, 123.19, 108.78, 107.91. FT-IR (ATR, cm$^{-1}$): 3395, 3310 ν(NH), 3056, 2938, 2890, 1586, 725. LC-MS (-ESI, *m/z*): 264.1 [M-2H]$^+$, 249, 194.4, 113.2, 69.0.

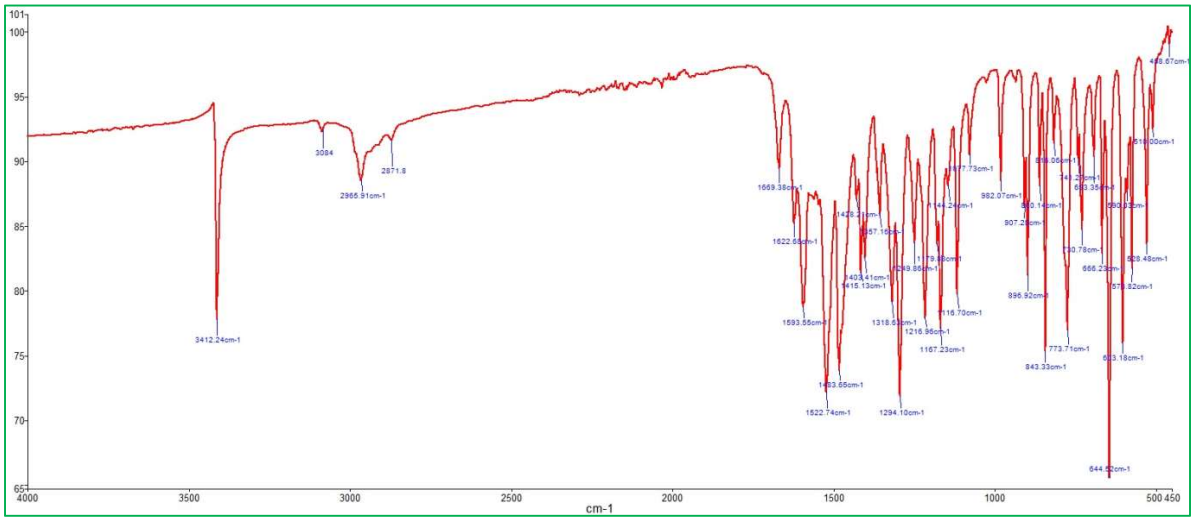


Figure 1. FT-IR spectra of the CBT.

### 2.3.4. Synthesis of *N*,*N*'-(((3,6-dichloro-9*H*-carbazole-1,8-diyl)*bis*(azanediyl))*bis*(carbonthioyl))*bis*(2,2-dimethylpropanamide) (CBT)

A solution of pivaloyl chloride (5 mmol) in dry acetone (50 mL) was added dropwise to a suspension of potassium thiocyanate (5 mmol) in acetone (30 mL). The reaction mixture was heated under reflux for 30 min, and then cooled to room temperature. A solution of 3,6-dichloro-9*H*-carbazole-1,8-diamine (5 mmol) in acetone (10 mL) was added and the resulting mixture was stirred for 2 h. After, the reaction mixture was poured into hydrochloric acid (0.1 N, 300 mL), and the solution filtered. The solid product was washed with water and dried (Scheme 1). Color: Grey. Yield: 75%. $^{1}$H NMR (400 MHz, DMSO-$d_6$, δ, ppm): 12.29 (s, 2H, NH), 11.40 (s, 1H, NH), 10.85 (s, 2H, NH), 8.31 (d, 2H, Ar-H), 7.55 (d, 2H, Ar-H), 1.29 (s, 18H, $CH_3$). $^{13}$C NMR (100 MHz, DMSO-$d_6$, δ, ppm): 181.72 (C=S), 179.86 (C=O), 134.80, 128.87, 125.31, 124.67, 123.87, 123.02, 122.84, 119.27, 26.27. FT-IR (ATR, cm$^{-1}$): 3395, 3310 ν(NH), 3056, 2938, 2890, 1586, 725.

### 2.3.5. Synthesis of co-crystal

*N*,*N*′-(((3, 6-Dichloro-9*H*-carbazole-1, 8-diyl)*bis* (azanediyl))*bis*(carbonothioyl))*bis*(2, 2-dimethyl-propanamide) were dissolved in 15 mL of acetic acid and heated at 100 °C for 30 min. After ten days yellow plates of the CBT:AcOH (1:1) co-crystal were obtained at room temperature. Color: Grey. Yield: 75%. $^{1}$H NMR (400 MHz, DMSO-$d_6$, δ, ppm): 12.30 (s, 2H, NH), 11.90 (s, 1H, OH), 11.40 (s, 1H, NH), 10.86 (s, 2H, NH), 8.30 (d, 2H, Ar-H), 7.56 (d, 2H, Ar-H), 1.92 (s, 3H, AcOH-$CH_3$), 1.29 (s, 18H, CBT-$CH_3$). $^{13}$C NMR (100 MHz, DMSO-$d_6$, δ, ppm): 181.64 (C=S), 179.77 (C=O), 171.79 (C=O, AcOH), 134.73, 125.22, 124.59, 123.79, 122.93, 119.19, 26.19, 20.91.

## 3. RESULT AND DISCUSSION

### 3.1. Spectral characterization

Precursor materials 3,6-dichlorocarbazole (1), 3,6-dichloro-1,8-dinitrocarbazole (2) and 1,8-diamino-3,6-dichlorocarbazole (3) were prepared according to the previously published method and characterized by FT-IR, $^{1}$H NMR, $^{13}$C NMR and LC/MS technique. The obtained results are in agreement with the previously published literature [27-29].

The CBT compound has been synthesized by reaction of pivaloyl chloride with an equimolar amount of potassium thiocyanate and 1,8-diamino-3,6-dichlorocarbazole in dry acetone and characterized by FT-IR, $^{1}$H NMR and $^{13}$C NMR spectroscopic techniques. The compound CBT shows characteristic sharp peaks in FT-IR spectrum due to ν(N-H), ν(C=O) and ν(C=S) stretching vibration modes at 3412, 1669 and 1294 cm$^{-1}$, respectively. The stretching vibration bands at 3084, 2955 and 2875 cm$^{-1}$ correspond to stretching of ν($C_{sp}^3$-H) and ν($C_{sp}^2$-H) groups of compound CBT (Figure 1).

In the $^{1}$H NMR spectrum of compound CBT, the signals for the $NH_{tiyoamide}$, the $NH_{pyrrole}$ and the $NH_{amide}$ protons are shown at the δ 12.31, 11.46 and 10.91 ppm, respectively. The signals for the aromatic protons in the compound CBT are observed at the δ 8.31 and 7.55 ppm as doublet. In addition, the singlet peak at δ 1.19 ppm seen in $^{1}$H NMR spectrum of compound CBT corres-ponds to $CH_3$ group (Figure 2). In $^{1}$H NMR spectrum of co-crystal, significant shifts were not observed for the above-mentioned groups. However, new signals from the acetic acid component of co-crystal have emerged at δ 11.90 ppm for -OH group as broad singlet peak and at δ 1.91 ppm for -$CH_3$ group as sharp singlet peak (Figure 2). In conclusion, it can be said that in the $^{1}$H NMR spectrum of co-crystal, CBT:AcOH molecular stoichiometry ration is 1:1.

In the $^{13}$C NMR spectrum of compound CBT, the signals for thiocarbonyl and carbonyl groups are shown at δ 181.72 and 179.86 ppm, respectively. The signals for the aromatic carbons are observed in the range of δ 119 and 134 ppm and the signals for the -$CH_3$ groups are shown at δ 26.19 ppm (Figure 3). The $^{13}$C NMR spectra of the co-crystal and CBT are almost the same. In addition to these signals in $^{13}$C NMR spectrum of the co-crystal, the new signals for carbonyl carbon and methyl group carbons of acetic acid component appeared at δ 171.79 and 20.91 ppm, repectively (Figure 3).

### 3.2. Molecular structure and conformation

Suitable crystals for X-ray analysis of co-crystal were obtained from glacial acetic acid. The co-crystal crystallizes in the monoclinic crystal system, space group $P2_1/c$ with $Z$ = 4 and in a 1:1 carbazole-based thiourea:acetic acid ratio. Further crystallographic data are presented in Table 1. Molecular structure of co-crystal is also presented in Figure 4.

Bond lengths and angles for CBT component of the co-crystal are presented in Table 2.

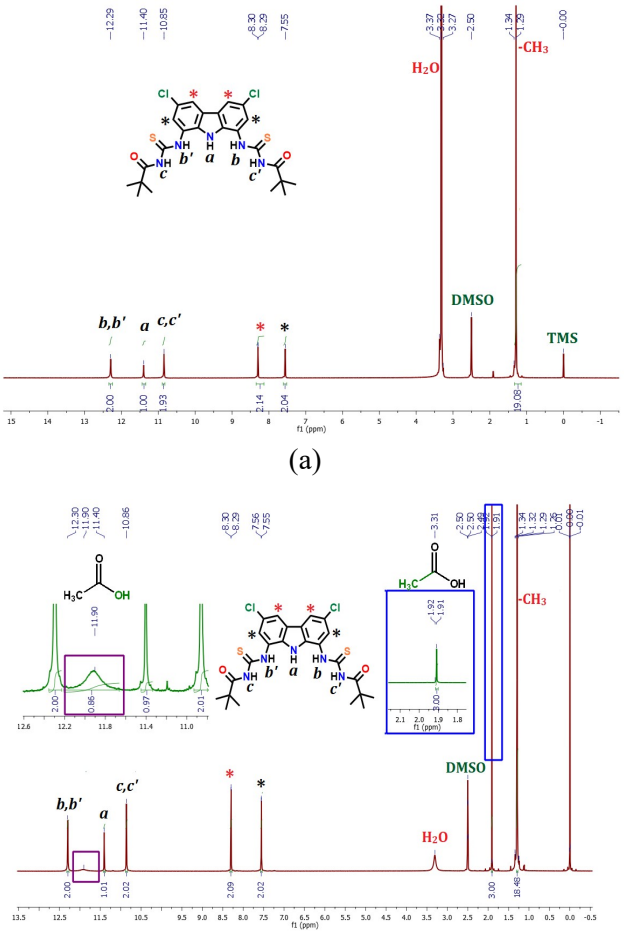


Figure 2. $^{1}$H NMR spectra of the CBT (a) and co-crystal (b) in DMSO-$d_6$.

The bond lengths of the thiocarbonyl and carbonyl groups in the CBT component are typical for double bonds, C13-S1 = 1.674(4), C19-S2 = 1.667(2), C14-O1 = 1.225(4) and C20-O2 = 1.228(4) Å. This difference between thio-carbonyl bond distances due to the intermolecular hydrogen bond between sulphur atom of CBT component and hydrogen atom of the AcOH component. The C-N bond lengths (N1-C1 = 1.386(4), N1-C12 = 1.386(5), N2-C2 = 1.430(5), N3-C14 = 1.386(5) Å, N3-C13 = 1.383(5) and N4-C11 = 1.427(4) Å) for the compound are all shorter than the average single C–N bond length and are all longer than the average double C–N bond length. These C-N bond lengths indicate a partial electron delocalization within the C(S)-NH-Ph$_{CBT}$-NH-Ph$_{CBT}$-NH-C(S) fragment. These results are in agreement with the expected delocalization in CBT component and confirmed by C2-N1-C1 = 129.2(3), C1-N2-C6 = 109.7(3) and C1-N1-C12 = 107.8(3) ° showing a $sp^2$ hybri-dization on the nitrogen atoms.

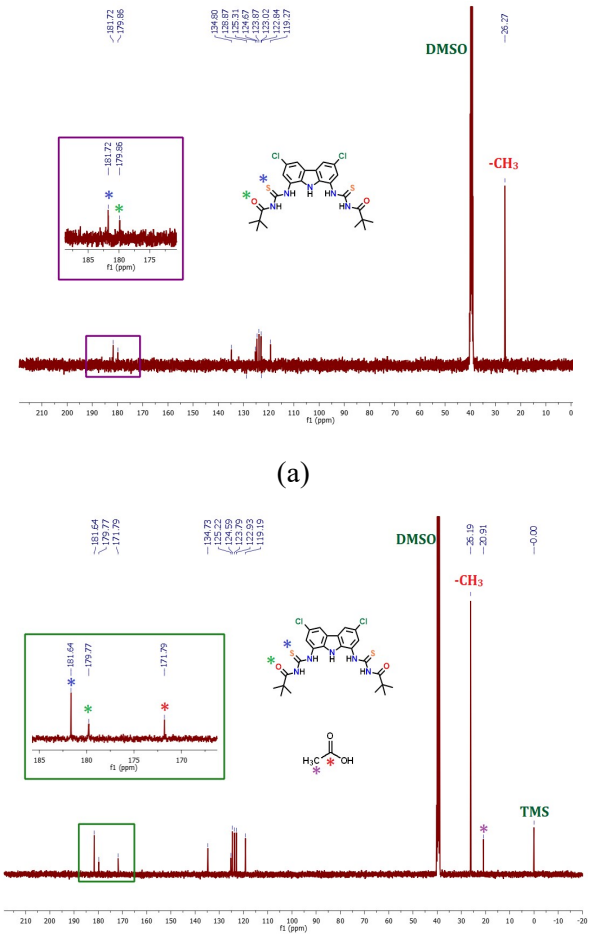


Figure 3. $^{13}$C NMR spectra of the CBT (a) and co-crystal (b) in DMSO-$d_6$.

In the co-crystal, the CBT component is stabilized by intramolecular hydrogen bonds, which are N2-H2···O1 and N4-H4···O2, with 1.92 and 1.93 Å bond distances, respectively (Figure 4). These hydrogen bonds cause the formation of two six-membered ring systems. Intra- and inter-mole-cular hydrogen bonds and geometrical parameters of C–H···π interactions for co-crystal are given in Tables 3 and 4, respectively.

On the other hand, the co-crystal has three kinds of hydrogen bond donors, which are N-H, O-H and C-H. The C-H donors are the C($sp^3$)-H donors of the methyl group while N-H donors are the amide group and N-H in pyrrole ring. The hydroxyl oxygen atom in the acetic acid molecule is a good donor atom for tiyocarbonyl

sulphur atom of the CBT component, while carbonyl oxygen atom in the acetic acid is an acceptor atom for methyl hydrogen of the CBT.

In co-crystal, there are two kinds of intermolecular interactions between the donor and the acceptor atoms. Firstly, the CBT and AcOH components in the asymmetric unit of the co-crystal are binding with each other *via* strong intermolecular hydrogen bonds O-H···S between the thiocarbonyl group of CBT component and hydroxyl hydrogen of AcOH component, with S···H distance of 2.33 Å with symmetry code: 1-*x,* 1-*y,* 1-*z* (Figure 5, Table 2). Secondly, within the crystal lattice, the AcOH component in the co-crystal lock carbazole-based thiourea mole-cules, forming additional three C-H···O intermo-lecular interactions (Figure 5, Table 3).

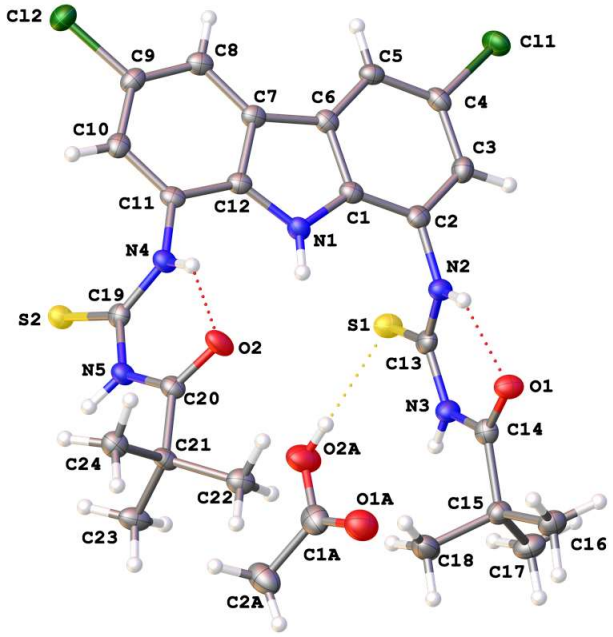


Figure 4. The structure of co-crystal, with labelling of atoms in the asymmetric unit and the formation of the six-membered ring system in CBT component via intramolecular hydrogen bonds.

Table 1. Crystal data and details of the structure refinement for co-crystal.

| **Parameters** | **Co-crystal** |
|---|---|
| Empirical formula | $C_{26}H_{31}Cl_2N_5O_4S_2$ |
| Formula weight | 612.58 |
| Temperature (K) | 103.97 |
| Crystal system | Monoclinic |
| Space group | $P2_1/c$ |
| a, (Å) | 8.8066(4) |
| b, (Å) | 16.3049(7) |
| c, (Å) | 20.6178(9) |
| β, (°) | 99.978(3) |
| Volume (Å$^3$) | 2915.7(2) |
| *Z* | 4 |
| $\rho_{calc}$ (g/cm$^3$) | 1.395 |
| μ (mm$^{-1}$) | 3.685 |
| F(000) | 1280.0 |
| Crystal size (mm$^3$) | 0.32 × 0.14 × 0.1 |
| Radiation | CuKα (λ = 1.54178) |
| 2Θ range for data collection (°) | 6.952 to 144.578 |
| Index ranges | $-10 \leq h \leq 10$, $-19 \leq k \leq 20$, $-25 \leq l \leq 24$ |

| | |
|---|---|
| Reflections collected | 34815 |
| Independent reflections | 5726 [$R_{int}$ = 0.2405, $R_{sigma}$ = 0.1018] |
| Data/restraints/parameters | 5726/0/361 |
| Goodness-of-fit on $F^2$ | 1.037 |
| Final R indexes [I≥2σ (I)] | $R_1$ = 0.0732, $wR_2$ = 0.1926 |
| Final R indexes [all data] | R1 = 0.0885, wR2 = 0.2132 |
| Largest diff. peak/hole / e Å$^{-3}$ | 0.69/-0.84 |

Table 2. Selected bond lengths (Å) and angles (°) of the co-crystal.

| **Atom** | | **Length (Å)** | **Atom** | | | **Angle (°)** |
|---|---|---|---|---|---|---|
| Cl(1) | C(4) | 1.743(4) | C(1) | N(1) | C(12) | 107.8(3) |
| Cl(2) | C(9) | 1.739(4) | C(13) | N(2) | C(2) | 121.1(3) |
| S(1) | C(13) | 1.674(4) | C(13) | N(3) | C(14) | 127.2(3) |
| S(2) | C(19) | 1.667(4) | C(19) | N(4) | C(11) | 125.2(3) |
| O(1) | C(14) | 1.225(4) | N(1) | C(1) | C(2) | 129.2(3) |
| O(2) | C(20) | 1.228(4) | N(1) | C(1) | C(6) | 109.7(3) |
| N(1) | C(1) | 1.386(4) | N(1) | C(12) | C(7) | 110.2(3) |
| N(1) | C(12) | 1.386(5) | N(1) | C(12) | C(11) | 128.7(3) |
| N(2) | C(2) | 1.430(5) | C(11) | C(12) | C(7) | 121.1(3) |
| N(2) | C(13) | 1.340(5) | N(2) | C(13) | S(1) | 122.7(3) |
| N(3) | C(13) | 1.383(5) | N(2) | C(13) | N(3) | 116.7(3) |
| N(3) | C(14) | 1.386(5) | N(3) | C(13) | S(1) | 120.6(3) |
| N(4) | C(11) | 1.427(4) | O(1) | C(14) | N(3) | 120.9(3) |

Table 3. Intra- and inter-molecular hydrogen bonds for co-crystal (Å,°) *.

| **D-H···A** | **d(D-H)** | **d(H···A)** | **d(D···A)** | **∠ (D-H···A )** |
|---|---|---|---|---|
| N(1)-H(1)···S(2) *i* | 0.88 | 2.67 | 3.418(3) | 144 |
| N(1)-H(1)···O(1) *ii* | 0.88 | 1.92 | 2.595(4) | 133 |
| O(2A)-H(24)···S(1) *ii* | 0.84 | 2.33 | 3.172(4) | 176 |
| N(3)-H(3)···O(1A) *iii* | 0.88 | 2.23 | 3.076(5) | 157 |
| N(4)-H(4)···O(2) | 0.88 | 1.93 | 2.630(4) | 136 |
| N(2)-H(2)···O(1) | 0.88 | 1.92 | 2.595(4) | 135 |
| C(2A)-H(2AB)···O(1) *iii* | 0.98 | 2.55 | 3.323(5) | 136 |
| C(18)-H(18C)···O(1A) *ii* | 0.98 | 2.56 | 3.469(6) | 154 |
| C(24)-H(24C)···S(1) *i* | 0.98 | 2.83 | 3.780(4) | 163 |

* Symmetry codes for co-crystal: *i* = 1-*x,* 1-*y,* 1-*z; ii* = *x*, -1+*y*, *z*; *iii*= -1+x, y, z.

Table 4. Geometrical parameters of C–H···π interactions for co-crystal (Å, °) [a].

| **C-H···Cg(J)** [b] | **H···Cg** | **H-perp** [c] | **∠C-H···Cg** | **γ** [d] | **C···Cg** [e] |
|---|---|---|---|---|---|
| C22-H22C···Cg(3) *i* | 2.68 | 2.65 | 141 | 8.63 | 3.500(4) |
| C23-H23A···Cg(1) *ii* | 2.75 | -2.75 | 117 | 3.01 | 3.313(4) |
| C23-H23C···Cg(3) *ii* | 2.73 | -2.68 | 133 | 11.41 | 3.475(4) |
| C24-H24A···Cg(1) *i* | 2.62 | 2.61 | 139 | 4.49 | 3.475(4) |

[a] Symmetry codes for co-crystal: *i* = 2-*x*,1-*y*,1-*z; ii* = 1-*x*,1-*y*,1-*z.* Cg(1) and Cg(3) are the centroids of the rings N1-C1-C6-C12 and C7-C12 of the CBT component, respectively.

[b] Center of gravity of ring J (Plane number above).

[c] Perpendicular distance of H to ring plane J.

[d] Angle between Cg-H vector and ring J normal.

[e] Distance between C-atom and the nearest carbon atom in the benzene ring.

In co-crystal, intermolecular interactions bond carbazole-based thiourea molecules to form a continuous one-dimensional chain through the *b* plane (Figure 5).

In the crystal structure, the CBT molecules are also linked by intermolecular hydrogen bonds. The N-H···O and N-H···S intermolecular hydrogen bond interactions form among the CBT molecules. These interactions cause the formation of molecular dimers, generating $R_2^2(12)$ and $R_2^2(14)$ homosynthons.

The N-H···O interactions occur between the tiyoamide hydrogen of CBT atom and the oxygen atom of carbonyl group, while N-H···S interactions form between the pyrrole amine of CBT and sulphur atom of the thiocarbonyl group. These motifs could play an important role in the stabilization of the co-crystal (Figure 6, Table 3).

In addition, the presence of trimethyl groups in CBT component lead to the presence of strong C-H···π intermolecular interactions which cause lattice stability. The dimeric entities between the CBT molecules are further supported through strong two type C-H···π intermolecular interactions.

The first occurs between the trimethyl group hydrogen atom and the phenyl ring of the carbazole skeleton, while the second one forms between the hydrogen atom of trimethyl group and the pyrrole ring of the carbazole skeleton. The crystal packing of the co-crystal is layered through these interactions (Figure 7, Table 4). All of these interactions construct a stable framework for co-crystal.

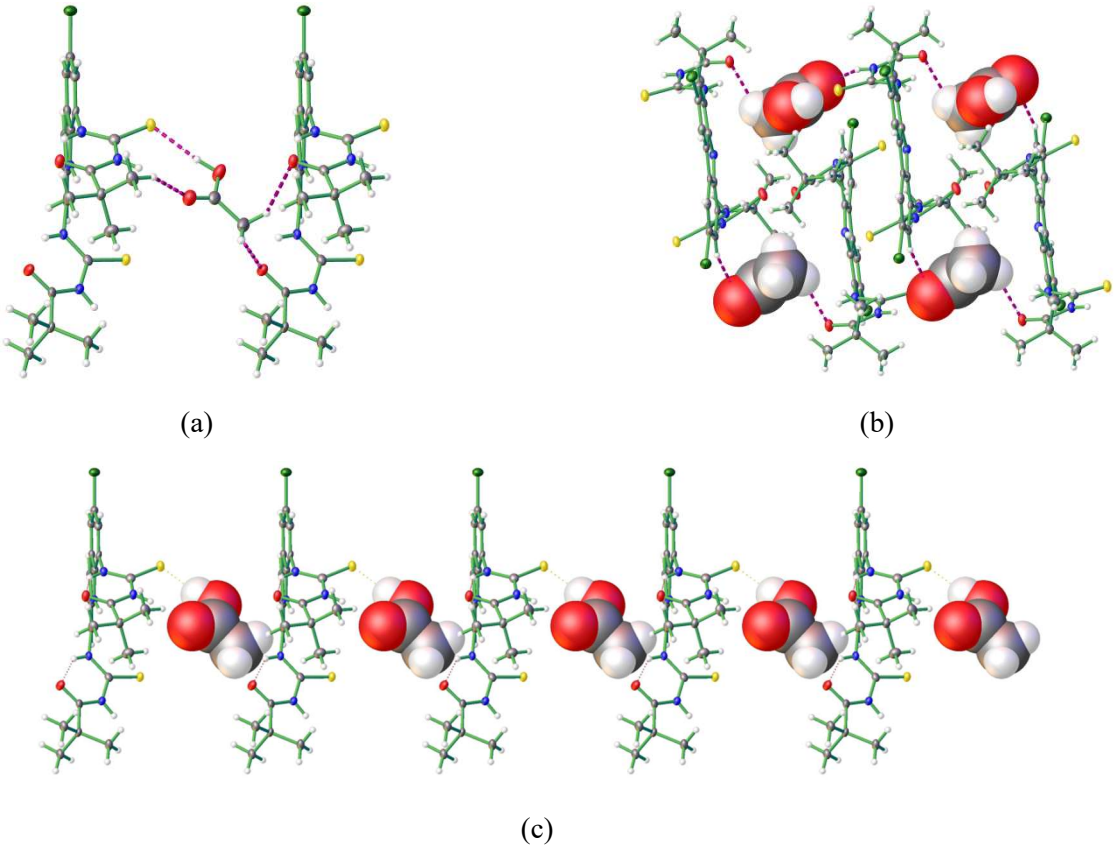

(a) (b)

(c)

Figure 5. (a) The O-H···S hydrogen bond and intermolecular C-O···H interactions in co-crystal, (b) the intermolecular interactions shown in space-filling representation of acetic acid, (c) the one-dimensional chain formed along the *b* direction.

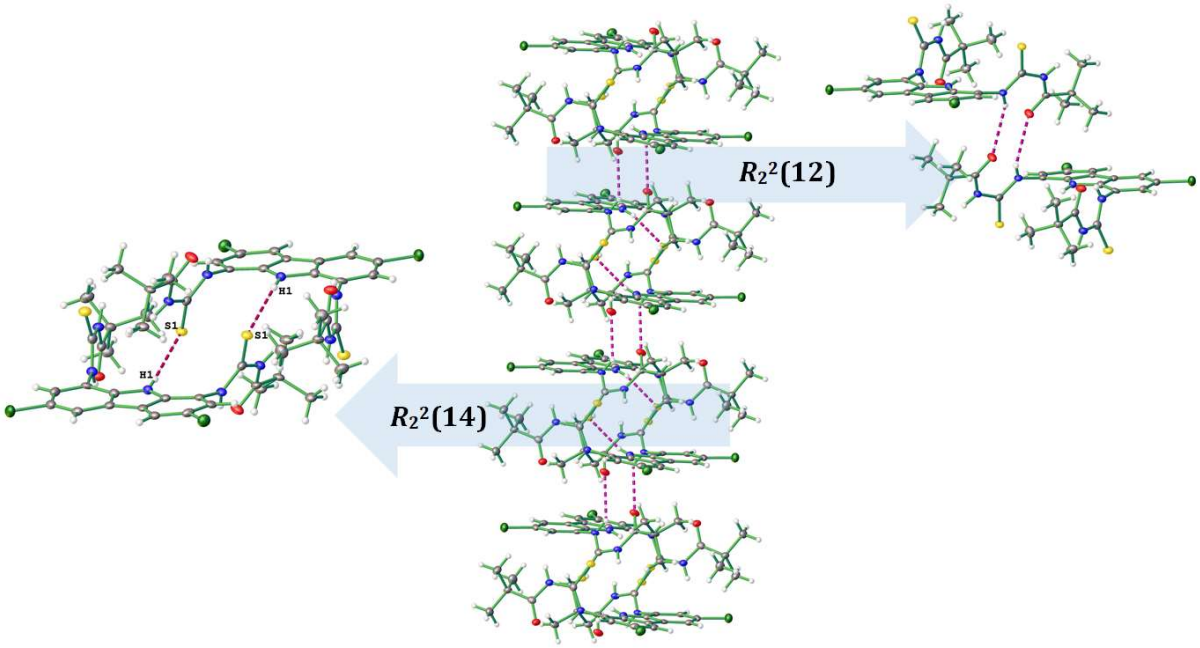


Figure 6. The formation of $R^2_2(12)$ and $R^2_2(14)$ synthon generated through N–H···S and N–H···O hydrogen bonds.

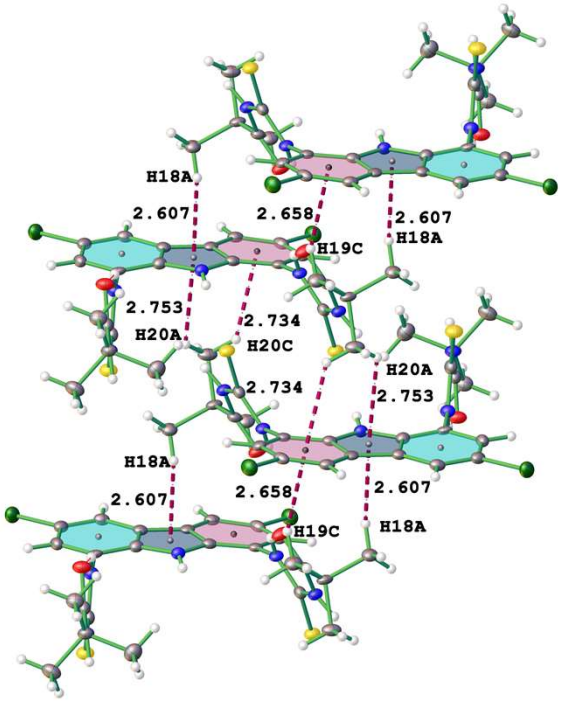


Figure 7. C-H···π interactions between CBT molecules of co-crystal.

### 3.3. Hirshfeld surface snalysis

The Hirshfeld surfaces of the co-crystal were analyzed to clarify the nature of the hydrogen bond interactions and close intermolecular interactions in the crystal structure and are illustrated by using the $d_{norm}$ and shape index Hirshfeld surface. In addition, all interactions were summarized by fingerprint plots. The Hirshfeld

surface mapped with $d_{norm}$ is the normalized contact distance, which is normalized from $d_e$ (the nearest external distance), $d_i$ (the nearest internal distance) and the van der Waals radii of the two atoms to the surface. The two dimensional fingerprint plot is derived from the Hirshfeld surface, these 2D fingerprint plots ensure a visual summary via combination of $d_i$ and $d_e$ across the surface of a molecule. In order to understand the interactions of the co-crystal, Hirshfeld surface calculations were performed on both CBT and AcOH crystals and all of the Hirshfeld surfaces were mapped over $d_{norm}$ and shape index.

The $d_{norm}$ surface of CBT molecule displays the close contacts of hydrogen bond donors and acceptors, but other close interactions are also evident. In $d_{norm}$ surfaces of the CBT molecule, the large red spots are signs of hydrogen bonding interactions whereas other visible spots are due to weaker interactions. The dominant C-S···H and N-H···O interactions are prominent in the Hirshfeld surface plots as the dark red area. The small and light color red areas on the surface indicates weaker and longer contacts other than hydrogen bonds between CBT molecules. An additional intramolecular C-H···Cl hydrogen bond in $d_{norm}$ surfaces of CBT molecule is observed as a weak red spot due to the presence of the chloro group (Figure 8). In the 2D fingerprint plots of CBT molecule, reciprocal strong S···H and H···O intermolecular interactions, with a contribution of 12.9 and 10.8%, respectively, appear as two distinct spikes. The region in the middle of the fingerprint plot represents the H···H interactions, with a contribution of 33.5%.

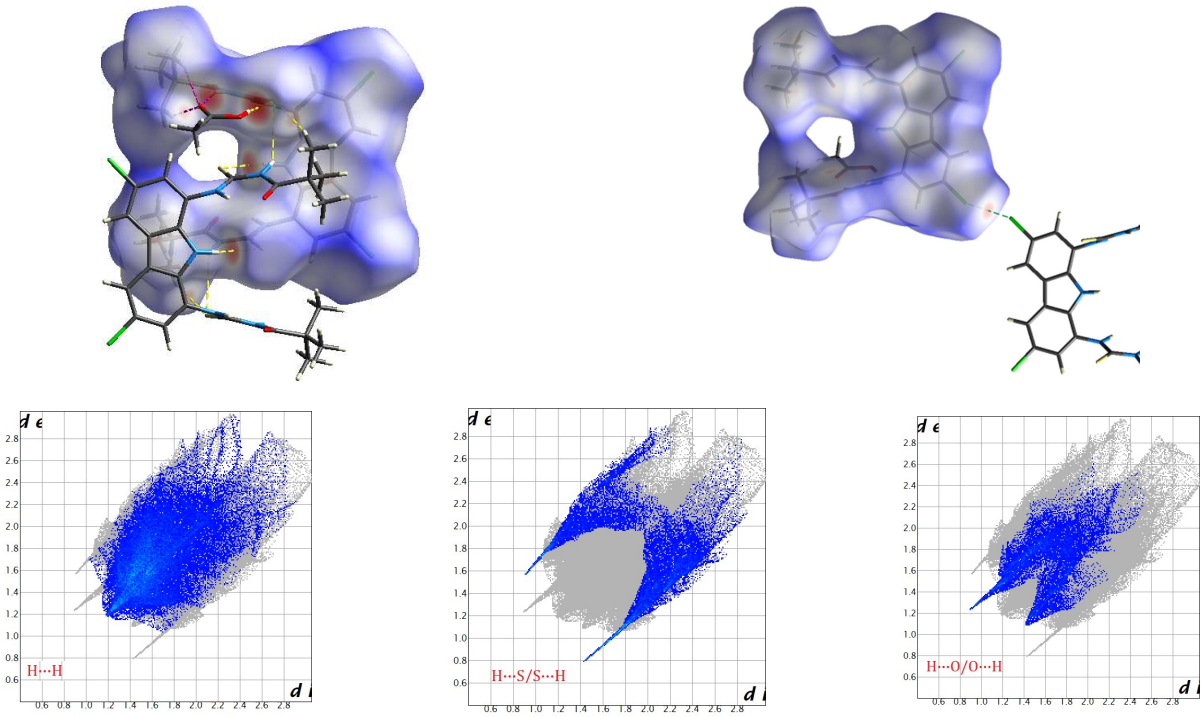


Figure 8. The Hirshfeld surface of the CBT mapped with $d_{norm}$ function and decomposed fingerprint plots showing relative contributions of reciprocal H···H, S···H and O···H intermolecular interactions.

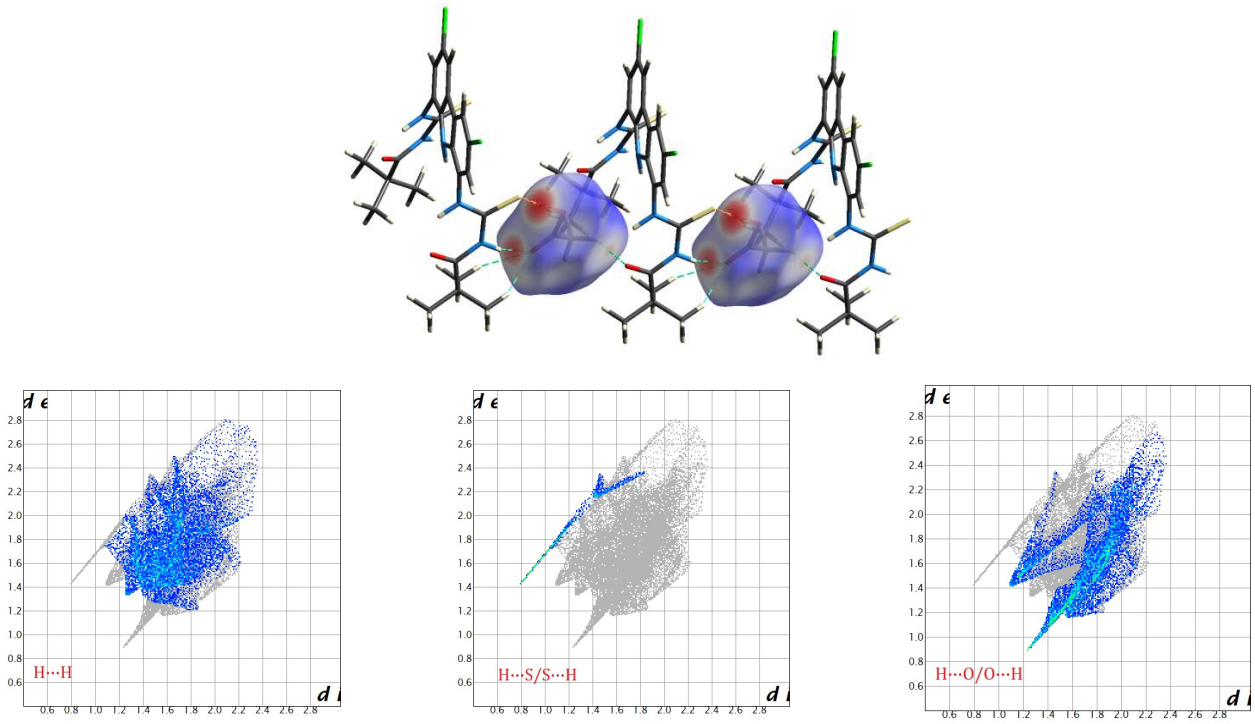


Figure 9. The Hirshfeld surface of the AcOH component in the co-crystal mapped with $d_{norm}$ function and decomposed fingerprint plots showing relative contributions of reciprocal H···H, S···H and O···H intermolecular interactions.

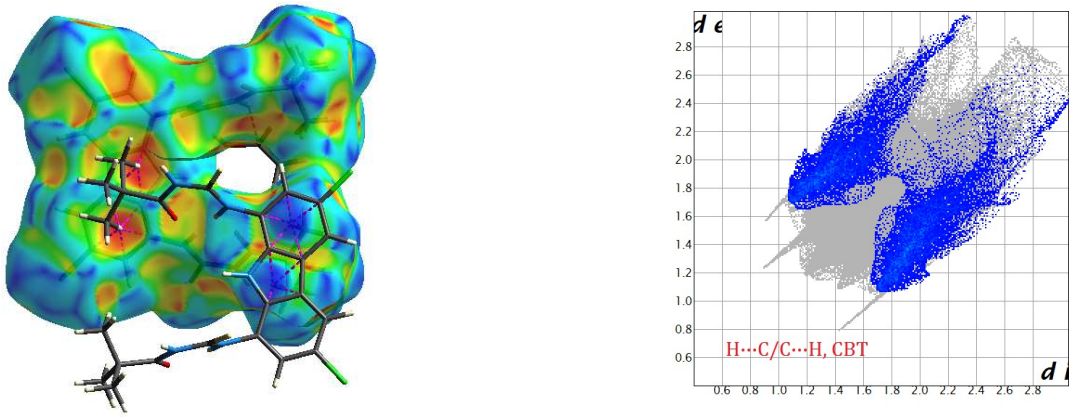


Figure 10. The Hirshfeld surface of the CBT mapped with shape index function and decomposed fingerprint plot showing relative contribution of reciprocal C···H intermolecular interactions.

The Hirshfeld surface analysis of the AcOH molecule reveals C-S···H and N-H···O interactions, which can be seen on the Hirshfeld surfaces as dark red spots corresponding to the short S···H and H···O contacts, respectively (Figure 9). The other light red spot on the Hirshfeld surface are caused by weak C-H···O contacts. The strong S···H/H···S intermolecular interactions, with a contribution of 5.2%, appear as one spike in the 2D fingerprint plot while the strong O···H/H···O intermolecular interactions, appear as two distinct spikes with a contribution of 39.7%. The H···H interactions in AcOH contain 42.9% of the total Hirshfeld surfaces and are intensely visible in the middle of the fingerprint plot.

The shape index Hirshfeld surface can be generally used to assign characteristic packing modes, planar stacking arrangements, and the ways in which neighboring molecules contact one another. The hollow red and bulging blue areas on the shape index surface of CBT molecule shows that the C-H···π

stacking interactions are dominant identical in the total crystal structures (Figure 10). These regions on the shape index surface are characteristic of C-H···π stacking interactions. These interacions contain 42.9% of the total Hirshfeld surfaces and are visible as "wing" in the fingerprint plot.

## 4. CONCLUSIONS

In this study, *N*,*N*′-(((3,6-dichloro-9*H*-carbazole-1, 8-diyl)*bis*(azanediyl))*bis*(carbonothioyl))*bis*(2, 2-dimethylpropanamide) as a carbazole-based thiourea derivative has been prepared. This compound was obtained in powder form due to its low solubility in many solvents. For a detailed analysis of the molecular structure of the compound, we wanted to obtain it in crystalline form by increasing solubility. For this reason, we aimed to make the compound soluble by increasing interactions between the molecules in the compound.

To achieve this purpose, we have prepared a new supramolecular cocrystal containing 1:1 ratio of the CBT and acetic acid, increasing intermole-cular interactions. So, the obtained co-crystal was characterized by single crystal X-ray analysis and molecular structure was examined in terms of supramolecular interactions. The structure deter-mination shows that the co-crystal is primarily stabilized by strong O–H···S hydrogen bonding and C-H···O interactions between the components of co-crystal. The co-crystal is also stacked in a parallel fashion, forming a layered 3D structure held together by C-H···π stacking interactions forming between molecules of CBT component. These supramolecular interactions observed by X-ray single crystal diffraction analysis were also examined by using Hirshfeld surface analysis and related fingerprint plots and reveal that the structure is stabilized by H···H, O–H···S, C–H···O and C–H···π intermolecular interactions.

## ACKNOWLEDGMENTS

This work was supported by the Mersin University Research Fund [Project No: 2016-AP4-1426]. This academic work was linguistically supported by the Mersin Technology Transfer Office Academic Writing Center of Mersin University.

## SUPPORTING INFORMATION

CCDC-1841129 contains the supplementary crystallographic data for this paper. These data can be obtained free of charge via https://www.ccdc.cam.ac.uk/structures/, or by e-mailing data_request@ccdc.cam.ac.uk, or by contacting The Cambridge Crystallographic Data Centre, 12 Union Road, Cambridge CB2 1EZ, UK; fax: +44(0)1223-336033.

## DISCLOSURE STATEMENT

Conflict of interests: The author declare that she has no conflict of interest.
Ethical approval: All ethical guidelines have been adhered.
Sample availability: Samples of the compounds are available from the author.

## ORCID

http://orcid.org/0000-0002-9398-0057

## REFERENCES

[1]. C. J. Janiak, "A critical account on π–π stacking in metal complexes with aromatic nitrogen-containing ligands," *Journal of the Chemical Society, Dalton Transactions*, vol. 21, pp. 3885-3896, 2000.

[2]. G. R. Desiraju, "C–H···O and other weak hydrogen bonds. From crystal engineering to virtual screening," *Chemical Communications*, vol. 24, pp. 2995-3001, 2005.

[3]. K. Thanigaimani, N. C. Khalib, E. Temel, S. Arshad and I. A. Razak, "New supramo-lecular co-crystal of 2-amino-5-chloro-pyridine with 3-methylbenzoic acids: Synt-heses, structural characterization, Hirshfeld surfaces and quantum chemical investiga-tions," *Journal of Molecular Structure*, vol. 1099, pp. 246-256, 2015.

[4]. L. Wang, R. A. Friesner and B. J. Berne, "Correction to "Replica Exchange with Solute Scaling: A More Efficient Version of Replica Exchange with Solute Tem-pering (REST2),"

*The Journal of Physical Chemistry B*, vol. 114, pp. 7294-7309, 2010.

[5]. P. A. Wood, F.H. Allen and E. Pidcock, "Hydrogen-bond directionality at the donor H atom—analysis of interaction energies and database statistics," *CrystEngComm*, vol. 11, pp. 1563-1571, 2009.

[6]. G. R. Desiraju,"Reflections on the Hydro-gen Bond in Crystal Engineering," *Crystal Growth & Design*, vol. 11, pp. 896-898, 2011.

[7]. K. Aoki, M. Nakagawa, T. Seki and K. Ichimura, "Self-assembly of amphoteric azo-pyridine carboxylic acids II: aspect ratio control of anisotropic self-assembled fibers by tuning the π– π stacking interac-tion," *Bulletin of the Chemical Society of Japan*, vol. 75, 2533-2539, 2002.

[8]. M. Ma and D. Bong, "Determinants of Cyanuric Acid and Melamine Assembly in Water," *Langmuir*, vol. 27, 8841-8853, 2011.

[9]. J. Janczak, "Supramolecular solid-state architectures formed by co-crystallization of melamine and 2-, 3- and 4-chloro-phenylacetic acids," *Journal of Molecular Structure*, vol. 1125, pp. 493-502, 2016.

[10]. M. S. Cunha, C. E. P. Ribeiro, C. C. Correa and R. Diniz, "The Hirshfeld surface of three new isonicotinylhydrazine co-crystals: Comparison of hydrogen bonds and crystal structures," *Journal of Molecular Structure*, vol. 1150, pp. 586-594, 2017.

[11]. G. P. Stahly, "A survey of cocrystals reported prior to 2000," *Crystal Growth & Design*, Vol. 9, No. 10, pp. 4212-4229, 2009.

[12]. C. B. Aakeröy, M. E. Fasulo and J. Desper "Co-crystal or salt: does ıt really matter?," *Molecular Pharmaceutics*, Vol.4, No. 3, pp 317-322, 2007.

[13]. M. L. Peterson, M. B. Hickey, M. J. Zaworotko and Ö. Almarsson, " Expanding the scope of crystal form evaluation in pharmaceutical science," *Journal of Pharmaceutical Sciences*, Vol.9, No. 3, pp 317-326, 2006.

[14]. E. Nauha, E. Kolehmaninen and M. Nissinen, "Packing incentives and a reliable N–H/N–pyridine synthon in co-crystal-lization of bipyridines with two agro-chemical actives," *CrystEngComm*, vol. 13, No. 21, pp. 6531-6537, 2011.

[15]. B. Chattopadhyay, S. Ghosh, S. Mondal, M. Mukherjee and A. K. Mukherjee, "Structural study of three o-hydroxy-acetophenone derivatives using X-ray powder diffraction: interplay of weak intermolecular interactions," *CrystEng Comm*, vol. 14, No. 3, pp. 837-846, 2012.

[16]. H. G. Brittain, "Co-crystal systems of pharmaceutical ınterest: 2011," *Crystal Growth & Design*, Vol. 12, pp. 5823-5832, 2012.

[17]. N. J. Babu and A. Nangia, "Solubility advantage of amorphous drugs and pharma-ceutical cocrystals," *Crystal Growth & Design*, Vol. 11, No. 7, pp. 2662-2679, 2011.

[18]. R. Thakuria, A. Delori, W. Jones, M. P. Lipert, L. Roy and N. Rodriguez-Hornedo, "Pharmaceutical cocrystals and poorly soluble drugs," *International Journal of Pharmaceutics*, Vol. 453, pp. 101–125, 2013.

[19]. R. Czerwonka, K. R. Reddy, E. Baum, H. J. Knölker, "First enantioselective total synt-hesis of neocarazostatin B, determination of its absolute configuration and transforma-tion into carquinostatin A," *Chemical Communication*, Vol. 0, pp. 711−713, 2006.

[20]. R. Forke, M. P. Krahl, T. Krause, G. Schlechtingen, H. J. Knölker, "Transition metals in organic synthesis, part 82. First total synthesis of methyl 6-methoxy-carbazole- 3-carboxylate, glycomaurrol, the anti-TB active micromeline, and the furo[2,3-c] carbazole alkaloid eustifoline-D," *Synlett*, Vol. 2, pp. 268−272, 2007.

[21]. O. V. Dolomanov, L.J. Bourhis, R.J. Gildea, J.A.K. Howard, H. Puschmann. J. Appl. Cryst. 42 (2009) 339-341.

[22]. L. Palatinus and G. Chapuis, *Journal of Applied Crystallography,* Vol. 40, pp. 786-790, 2007.

[23]. L. Palatinus, A. van der Lee. , *Journal of Applied Crystallography*, Vol. 41, pp. 975-984, 2008.

[24]. L. Palatinus, S. J. Prathapa. S. van Smaalen *Journal of Applied Crystallography,* Vol. 45, pp. 575-580, 2012.

[25]. G. M. Sheldrick, Acta Cryst. C71 (2015) 3-8. Vol. C71, pp. 3-8, 2015.

[26]. M. J. Turner, J. J. McKinnon, S. K. Wolff, D. J. Grimwood, P. R. Spackman, D. Jayatilaka, M. A. Spackman, Crystal Explorer17, University of Western Australia, 2017.

[27]. P. A. Gale, "Synthetic indole, carbazole, biindole and indolocarbazole-based recep-tors: applications in anion complexation and sensing," *Chemical Communication*, Vol. 0, pp. 4525-4540, 2008.

[28]. H. Arslan, "Metal katalizli oksidasyon reaksiyonları için ligand tasarım çalış-maları". TUBITAK, Proje no: 112T322, (2012).

[29]. I. Gumus, "Yeni Karbazol Türevi Redoks Aktif Ligandların ve Metal Kompleks-lerinin Sentezi ve Karakterizasyonu", Mersin Üniversitesi Fen Bilimleri Enstitüsü, Doktora Tezi, (2014).